Reconciling Order, Stability, and Porosity in Phosphonate Metal-Organic Frameworks via HF-mediated Synthesis

Journal:	*Inorganic Chemistry Frontiers*
Manuscript ID:	QI-RES-11-2014-000209.R1
Article Type:	Research article
Date Submitted by the Author:	16-Jan-2015
Complete List of Authors:	Mah, Roger; University of Calgary, Chemistry Gelfand, Benjamin; University of Calgary, Chemistry Taylor, Jared; Kyoto University, Shimizu, George; University of Calgary, Department of Chemistry

Cite this: DOI: 10.1039/c0xx00000x

www.rsc.org/xxxxxx

ARTICLE TYPE

Reconciling Order, Stability, and Porosity in Phosphonate Metal-Organic Frameworks via HF-mediated Synthesis

Roger K. Mah,[a] Benjamin S. Gelfand,[a] Jared M. Taylor,[a] and George K.H. Shimizu[a]*

Received (in XXX, XXX) Xth XXXXXXXXX 20XX, Accepted Xth XXXXXXXXX 20XX

DOI: 10.1039/b000000x

We report two porous Zr phosphonate frameworks. The kinetic product, ZrH_2L-A, shows low order and is less porous. An HF-modulated structure, CALF-31, is more ordered and has higher porosity. While not single crystalline, CALF-31 is highly robust and the CO_2 heats of adsorption give insights to ordering in phosphonate MOFs.

In the formation of porous network solids, the sustaining interactions pay the energetic cost of forming a void in the material. Metal organic frameworks (MOFs) are notable in part because of their ability to merge porosity with a highly crystalline architecture. Stability to the removal of guest molecules to enable reversible gas sorption constitutes one level of robustness. Higher degrees of robustness are desirable for targeted applications so stronger bonding than divalent cations with monoanionic carboxylates are needed.

One of the hallmark properties of MOFs is their crystallinity. For a solid to order during the self-assembly process, the balance between complex formation in solution and complex precipitation must allow some reversibility. With weakly interacting components (e.g. H-bonded salts), ordering of the solid is simple but sustaining pores in such a solid is a challenge. Recently, a focus in MOF chemistry has shifted to frameworks based on zirconium(IV) carboxylates as they show increased robustness largely due to the enhanced electrostatic interactions offered by the Zr^{4+} ion; these frameworks offer a means of balancing porosity, crystallinity, and stability. UiO-66 is often used as the benchmark for robustness and consists of $Zr_6O_4(OH)_4$ clusters connected by terephthalates.[1] UiO-66 had an unprecedented degree of both thermal and hydrolytic stability for a MOF and now other frameworks show similar degrees of stability.[2–5]

Phosphonate linkers can form stronger bonds to metals than carboxylates resulting in robust frameworks[6] but often at the expense of crystallinity. Zirconium phosphonates tend to adopt a dense layered motif such as in α-zirconium phosphonates where ZrO_6 octahedra are linked by R-PO_3 tetrahedra[7]; each oxygen is bound to a different zirconium center and the R group on the phosphonate points into the interlayer space. By using linear diphosphonates, pillared-layered materials are obtained in the absence of structure-directing agents.[8] These two trends of low crystallinity and a tendency towards pillared-layered structures often make rational design of porous phosphonate MOFs a difficult, but not impossible, task. In this vein, enhancing the bond strength between the organic and inorganic components using a divergent polyphosphonate with zirconium(IV) could target a porous and robust material. When trigonal triphosphonates are used, the typical layered motif is disfavoured as a consequence of the geometry of the linker; 1D inorganic chains linked by the trigonal ligand forming honeycomb pores are obtained.[9,10]

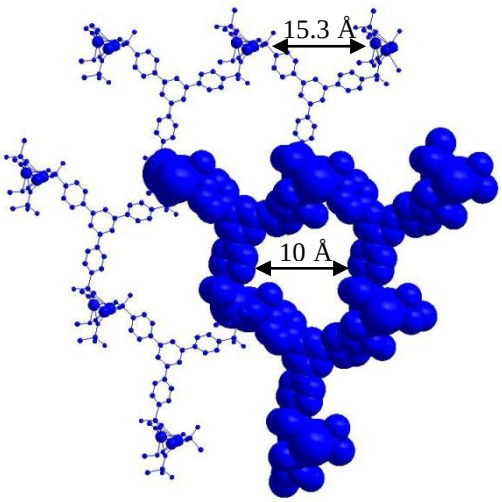

Figure 1: Crystal structure of a single net observed in SrH_4L. 15.3 Å d-spacing observed and shown between metal centers. 10 Å pores observed once van der Waals radii are accounted for.[8]

This motif was observed in our recently reported synthesis of SrH_4L (L = 1,3,5-tris(4-phosphonophenyl)benzene)[9] and CALF-28 (CALF=CALgary Framework).[11] SrH_4L consists of 1D PO_3-bridged Sr inorganic chains linked together with H_4L forming a honeycomb structure (**Figure 1**) with interpenetrated nets preventing the formation of significant void space. CALF-28 forms when tin(IV) coordinates H_2L. CALF-28 shows permanent porosity and high water stability but lacked long range order. The structure of CALF-28 was modelled off SrH_4L and consists of a similar topology but without an interpenetrated net, which allows for its high porosity.

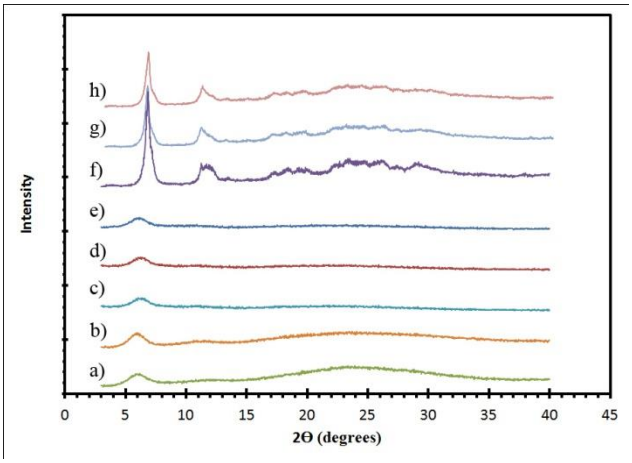

Figure 2: PXRD patterns for different synthesis conditions towards the final synthesis of CALF-31. a) ZrH_2L-A from room temperature precipitation; b) ZrH_2L-A after 48 hour humidity exposure; c) reflux synthesis; d) hydrothermal synthesis at 120 ℃ for 48 hours; e) HCl addition to hydrothermal synthesis; f) 48% HF hydrothermal synthesis at 150 ℃ for 120 hours; g) CALF-31; h) CALF-31 after 24 hours of humidity exposure.

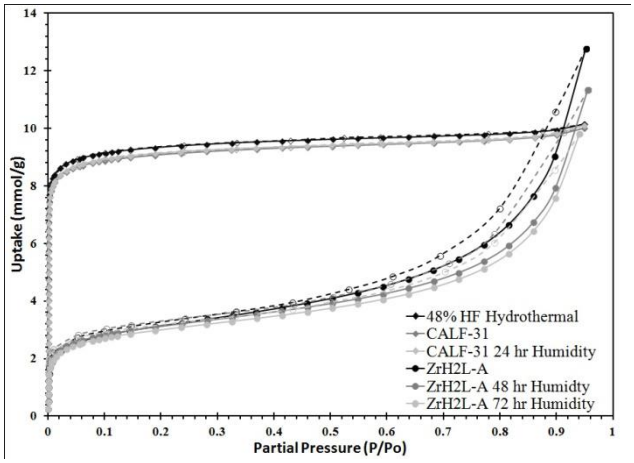

Figure 3: N_2 isotherms at 77 K for different humidity treatments. ZrH_2L-A isotherms are in teal while CALF-31 isotherms are in black.

Herein we present solvothermal reaction of H_6L and zirconium(IV) to give two porous forms of ZrH_2L $(H_2O)_7$. One is an amorphous material, ZrH_2L-A, and the other is a semi-crystalline framework, CALF-31. ZrH_2L-A is permanently porous with a surface area <300 m^2/g but lacks order as result of its kinetic formation. A range of synthetic methods are employed to enhance the order in this system to form CALF-31, a microcrystalline, highly robust MOF with a surface area of ~800 m^2/g.

While no single crystal structure of CALF-31 is presented, iterative improvements to the synthesis allow for sufficient order to gauge structural features. Porosity and crystallinity are retained even after exposure to harsh humidity conditions (85 ℃ and 95% RH). CALF-31 offers porosity and high stability at the cost of some crystallinity, ultimately a strategy for generating a functional material.

H_6L was prepared by reported methods,[11] ZrH_2L-A was prepared by room temperature precipitation, and CALF-31 was synthesized by solvothermal reaction. The details of these syntheses can be found in the supporting information. The synthesis of CALF-31 and characterization required varied approaches and gathering data from multiple pieces to determine the structure and formula. We used the previously reported SrH_4L as a model for the structure determination of CALF-31. Reaction conditions that enable kinetic reversibility of the metal-linker self-assembly are required to obtain an ordered structure. Different conditions were tested to enhance order in CALF-31.

The initial condition pursued involved room temperature mixing of $ZrCl_4$ and H_6L yielding ZrH_2L-A. Powder x-ray diffraction (PXRD) of the white powder obtained revealed an amorphous material with a broad low angle peak (**Figure 2**).

The molecular formula of ZrH_2L-A was determined as ZrH_2L $(H_2O)_7$ by energy-dispersive x-ray spectroscopy (EDX), elemental analysis (EA), and thermogravimetric analysis (TGA) (**SI Figure 1**). EDX revealed a P/Zr ratio of 2.9:1 (calc. 3:1) indicating a 1:1 ratio of L to Zr in the product. EA gave 38.0% carbon and 3.7% hydrogen in agre**e**ment with the theoretical values (calc. 38.0% and 4.1%). A mass loss of 12% (calc.17%) from 20-100 ℃ corresponds to a loss of 4.5 water molecules. The inconsistency between TGA and EA can be accounted for by loss of water due to time elapsed between EA and TGA.

ZrH_2L-A was examined for porosity and stability to humidity. It was porous giving a maximum N_2 uptake at 77 K of 12.8 mmol/g. The isotherm shape is type 1 with tailing into a type 2 showing multilayer growth (**Figure 3**). The associated BET surface area was 253 m^2/g (Langmuir, 299 m^2/g). A t-plot analysis partitioned the micropore region as 93 m^2/g and the external surface as 160 m^2/g. A bimodal pore distribution was modelled using non-local density functional theory (NLDFT) giving maxima at 8 and 14 Å (**Figure 4**). The CO_2 uptake of ZrH_2L-A at 1200 mbar was 1.45 mmol/g at 263 K and 1.28 mmol/g at 273 K (**Figure 5**).

The water stability of ZrH_2L-A was assessed by 24, 48, and 72 hour exposures to 85 ℃ and 95% RH and the structure and gas uptake of the solid revisited. These results showed that the treatments induce a structural change in the material, not surprising giving the amorphous product was precipitated at ambient conditions. The initial 24 hours of exposure resulted in a 19.4% decrease in BET surface area from 253 m^2/g to 204 m^2/g and a 30.3% decrease CO_2 uptake at 1200 mbar from1.45 mmol/g to 1.03 mmol/g. After 48 hours of exposure, ZrH_2L-A showed a recovery and even a slight increase in BET surface area to 253 m^2/g (Langmuir, 299 m^2/g) (**SI Figure 2**). The CO_2 showed a slight increase in uptake at 1.58 mmol/g at 263 K and 1.40 mmol/g at 273 K (**SI Figure 3**). After 72 hours, there was a slight decrease in BET surface area to 244 m^2/g (Langmuir, 288 m^2/g). The microporosity is actually enhanced after humidity treatment to 106 m^2/g with an external surface of 138 m^2/g. The CO_2 also mirrored this slight decrease with values of 1.50 mmol/g at 263 K and 1.33 mmol/g at 273 K (**SI Figure 4**). The zero-loading heats of adsorption (HOA) for CO_2 will be discussed with CALF-31.

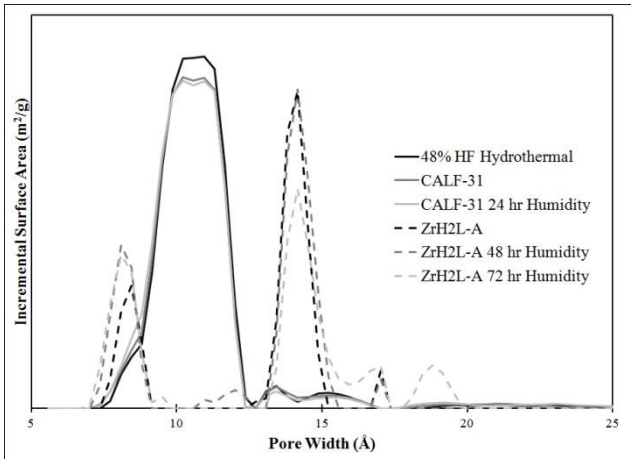

Figure 4: Pore distribution from NLDFT modelled off of the 77K N_2 isotherms. The bimodal ZrH_2L-A plots (8 and 14 Å) are in teal while the single apex CALF-31 plots (10 Å) are in black.

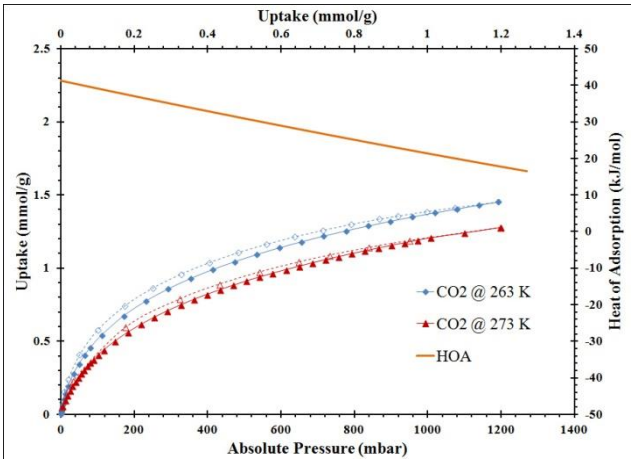

Figure 5: CO_2 isotherms at 263 K (blue) and 273 K (red) for ZrH_2L-A with the isosteric HOA (orange) on the secondary axis.

To increase the structural order of ZrH_2L-A, several other routes were attempted. A methanolic solution of H_6L was added dropwise to a refluxing solution containing $ZrCl_4$ in H_2O, however the product formed did not give any increased order. A series of solvothermal reactions were then attempted. $ZrCl_4$ (0.011 g, 0.047 mmol) and H_6L (0.025 g, 0.046 mmol) were dissolved in methanol (2 mL) and water (2 mL) then placed in a hydrothermal vessel and heated at 120 ℃ for 48 hours resulting in the formation of a thick white solution that, when filtered, gave a powder with no notable increase in crystallinity. The hydrothermal syntheses were repeated with the addition of HCl (0.04 mL, 0.46 mmol) to control pH and favor the protic form of the ligand but these also resulted in low degrees of order by PXRD (**Figure 2**).

Reversible reaction conditions of the metal-linker assembly are required to obtain the ordered structure in CALF-31. Therefore, a more soluble Zr precursor was postulated to increase kinetic reversibility, so ZrF_6^{2-} species were targeted. These syntheses required the use of HF. *HF is fatal if swallowed, inhaled or in contact with skin and will cause severe burns to the eyes, skin and respiratory tract.* Use of 48% HF was pursued for synthesis of CALF-31 and ultimately produced the most ordered and phase pure material. Changes to the temperature, duration, and equivalents of HF were employed in an attempt to further enhance the crystallinity but these variations resulted in either the same degree of order or decomposition of the ligand. The product obtained from the HF preparations was then exposed to 85 ℃ and 95% RH for 48 hours to obtain CALF-31. It should be noted that, for safety, preparations were carried out using NaF and HCl to generate HF in situ but these gave an intractable and significantly abundant impurity phase (**SI Figure 5**).

Single crystals of CALF-31 were never attainable so again a combination of characterization techniques, EDX, EA, and TGA (**SI Figure 6**) were required to determine the molecular formula as with ZrH_2L-A. The formula for CALF-31 was determined as $ZrH_2L(H_2O)_7$; the same formula assigned to ZrH_2L-A. EDX revealed a P:Zr ratio of 3.1:1, in good agreement with the calculated 3:1 and also confirmed the absence of F ions. EA gave 37.8% carbon and 3.6% hydrogen, (calc. 38.0%, 4.1%). The TGA showed a weight loss of 17% corresponding to 7 water molecules lost (calc. 17%).

With the molecular formula determined, a structure can be proposed by combining information from the model compound, SrH_4L, combined with PXRD and gas sorption. 1D honeycomb pores are expected in CALF-31 as a result of the pore geometry observed in SrH_4L. This type of assembly allows for the phosphonate coordination to Zr while also allowing the hydrophobic interactions between the ligand cores. The PXRD of CALF-31 (**Figure 2**) shows a low angle peak at 5.9° corresponding to a d-spacing of 15.0 Å representing the repeat spacing between metal centers across the honeycomb. This is slightly below the d-spacing observed in the SrH_4L (15.3 Å) structure as expected given the smaller radii for Zr^{4+}. The peaks are broadened and there is also a slight amorphous hump indicating that CALF-31 is not highly crystalline.

The porosity of CALF-31 was evaluated using a N_2 isotherm at 77K and CO_2 isotherms at 195, 263, 273, and 298K isotherms. The N_2 isotherm has a type I isotherm shape (**Figure 3**) as expected from a microporous material with 10.0 mmol/g uptake at 850 mbar corresponding to a BET surface area of 793 m^2/g (Langmuir, 879 m^2/g). A t-plot analysis partitioned this as 694 m^2/g and 99 m^2/g for micropore and external surface, respectively. The pore distribution modelled using NLDFT from the N_2 isotherm reveals a pore size of 10 Å (**Figure 4**). This is consistent with the pores observed in SrH_4L (10 Å) after accounting for van der Waals radii of the atoms on the periphery of the honeycomb. Notably, the distribution is no longer bimodal as in ZrH_2L-A although it is slightly broader. The CO_2 sorption was measured and at 1200 mbar the uptakes were 4.60 mmol/g at 263 K and 3.65 mmol/g at 273 K (**SI Figure 7**). The CO_2 capacity was tested on CALF-31 and showed an uptake of 9.31 mmol/g at 195 K and 820 mbar (**SI Figure 8**). To the best of our knowledge, this is the highest CO_2 capacity among phosphonate based MOFs at 820 mbar. Additionally, the

CO_2/N_2 selectivity was determined to be 13.0 at 298K (**SI Figure 9**). This is relatively low due to the low heat of adsorption of CO_2 to be discussed.

From CO_2 isotherms run at 263, 273 and 298K, the isosteric heats of adsorption for CO_2 were calculated using a Virial model for the different ZrH_2L-A and CALF-31. For ZrH_2L-A, the zero loading was 41 kJ/mol, indicating that there are high energy adsorption sites present, and decreased to 16 kJ/mol with increased CO_2 loading (**Figure 5**). The higher energy sites are likely exposed free phosphonate oxygen atoms that would polarize the CO_2 molecules. *Monodentate and bidentate phosphonate groups would be more prevalent in a less ordered material, as would result from the rapid precipitation at ambient conditions, versus a symmetrical tridentate coordination mode expected for the more ordered structures.* These free oxygen atoms are high energy polarising sites and interact strongly with CO_2 molecules. The rapid decline of the HOA indicates that these sites are not abundant. For the ZrH_2L-A sample that had been humidity treated for 48 hours, the zero-loading HOA was 36 kJ/mol and for the 72 hour sample, the zero-loading HOA dropped to 31 kJ/mol. For CALF-31 the CO_2 HOA values was 17 kJ/mol and increased to 24 kJ/mol with loading. This range is representative of a hydrophobic material and one with few exposed polarising oxygen atoms, consistent with tridentate coordination of the R-PO_3 groups and a more ordered solid.

Stability of CALF-31 was gauged by subjecting the sample to elevated temperature and humidity then assessing (1) retention of crystallinity and (2) change in porosity, if any. From the TGA, it is evident that CALF-31 is thermally stable with no evidence of decomposition up to 400 ℃. Between 400 - 800 ℃ there is a gradual decrease in mass until a large decomposition step observed above 800 ℃. CALF-31 was subjected to harsh humidity conditions (85 ℃, 95% RH) for 24 hours before being tested via PXRD and gas sorption to determine the stability. After 24 hours of exposure the PXRD remained unchanged. The N_2 isotherm showed minor changes after 24 hours of humidity treatment; the N_2 uptake was 10.1 mmol/g with a BET surface areas of 786 m^2/g (Langmuir, 882 m^2/g) (**Figure 3**). Again t-plot analysis gave 687 m^2/g and 100 m^2/g for micropore and external surface, respectively, close to the pristine MOF. The pore distribution remained unchanged with a single pore size of 10 Å (**Figure 4**). The CO_2 uptake was stable with uptakes of 4.63 mmol/g at 263 K and 3.70 mmol/g at 273 K with a HOA of 19 - 22 kJ/mol (**SI Figure 10**). From this it can be stated that CALF-31 is highly stable both thermally and against hydrolytic cleavage.

In ideal MOF research, a robust and porous structure is obtained with a single crystal matching bulk synthesis. It has seemed that if this ideal cannot be reached, it is preferable to obtain a crystalline product at the cost of robustness and function. While this facilitates dissemination, the ultimate utility of the material is undermined. In this work, we have sought a route to reconcile the desirable features with an emphasis on function than definitive structure. The result is a robust phosphonate with a significant degree of porosity. Moreover, the sequential modification and characterization of intermediate phases showed that the zero-loading heat of adsorption for CO_2 was a reasonable metric for the ordering of the solid owing to fewer dangling phosphonate groups. Recently, Taddei et al. published a related and highly crystalline framework, $Zr_3(H_3L)_4$, but, due to packing of layers in an ABA style to decrease void space, there was no N_2 porosity observed.12 Lin has previously reported amorphous Zr binaphthol phosphonates with surface areas < 600 m^2/g.[13] The semi-crystalline CALF-31 has, to the best of our knowledge, the highest surface area for a phosphonate framework to date.

Conclusions

Here we have reported the synthesis of $ZrH_2L(H_2O)_7$ as an amorphous ZrH_2L-A and a semi-crystalline CALF-31. ZrH_2L-A established a baseline of properties for comparison to CALF-31 to establish the changes incurred by increasing order. ZrH_2L-A is permanently porous with a BET surface area of 253 m^2/g. The CO_2 uptakes at 263 K and 273 K were 1.45 mmol/g and 1.28 mmol/g respectively corresponding to a HOA of 41 – 16 kJ/mol. CALF-31 was synthesized using a HF modulator. Using previously observed structures as models combined with PXRD, EA, EDX, and pore size distributions, it was determined that CALF-31 was $ZrH_2L(H_2O)_7$ with 10Å honeycomb pores. The surface area of CALF-31 is 793 m^2/g; the CO_2 uptakes are 4.60 mmol/g at 263 K and 3.65 mmol/g at 273 K giving a HOA of 17 – 24 kJ/mol. After humidity exposure at 85 ℃ and 95% RH, both ZrH_2L-A and CALF-31 show very slight decreases in surface area and CO_2 uptake but porosity is retained indicating high stability against hydrolytic cleavage of the frameworks.

Notes and references

Department of Chemistry, University of Calgary, 2500 University Dr NW, Calgary AB, T2N 1N4, Canada. Fax: +1 403 2899488; Tel: +1 403 2205347 Email: gshimizu@ucalgary.ca

† Electronic Supplementary Information (ESI) available: synthetic details, XRD, gas sorption analysis, SEM-EDX, TGA curves.

We acknowledge Carbon Management Canada for support of this research and Alberta Innovates Technology Futures for a graduate scholarship to BSG.

1. J. H. Cavka, S. Jakobsen, U. Olsbye, N. Guillou, C. Lamberti, S. Bordiga and K. P. Lillerud, *J. Am. Chem. Soc.*, 2008, **130**, 13850–13851.
2. G. Férey, C. Mellot-Draznieks, C. Serre, F. Millange, J. Dutour, S. Surblé and I. Margiolaki, *Science*, 2005, **309**, 2040–2042.
3. (a) V. Colombo, S. Galli, H. J. Choi, G. D. Han, A. Maspero, G. Palmisano, N. Masciocchi and J. R. Long, *Chem. Sci.*, 2011, **2**, 1311–1319. (b) A. Demessence, D. M. D'Alessandro, M. L. Foo and J. R. Long, *J. Am. Chem. Soc.* **2009**, *131*, 8784-8786.
4. (a) C. R. Wade, T. Corrales-Sanchez, T. C. Narayan and M. Dincă, *Energy Environ. Sci.*, 2013, **6**, 2172–2177. (b) T. Li, D. L. Chen, J. E. Sullivan, M. T. Kozlowski, J. K. Johnson and N. L. Rosi,. *Chem. Sci.* 2013, **4**, 1746-1755.
5. H. Jasuja, Y.-G. Huang and K. S. Walton, *Langmuir*, 2012, **28**, 16874–16880.
6. G. Alberti, M. Casciola, U. Costantino and R. Vivani, *Adv. Mater.*, 1996, **8**, 291–303.
7. (a) C. Serre, J. A. Groves, P. Lightfoot, A. M. Z. Slawin, P. A. Wright, N. Stock,T. Bein, M. Haouas, F. Taulelle, and G. Férey,

Chem. Mater., 2006, **18,** 1451. (b) S. R. Miller, G. M. Pearce, P. A. Wright, F. Bonino, S. Chavan, S. Bordiga, I. Margiolaki, N. Guillou, G. Férey, S. Bourrelly and P. L. Llewellyn, *J. Am. Chem. Soc*., 2008, **130**, 15967. (c) D. L. Lohse and S. C. Sevov, *Angew. Chem., Int. Ed. Engl*., 1997, **36**, 1619. (d) M. B. Dines; R. E. Cooksey, P. C. Griffith and R. H. Lane, *Inorg. Chem*., 1983, **22**, 1003. (e) K. Maeda, Y. Kiyozumi and F. Mizukami, *Angew. Chem., Int. Ed. Engl*., 1994, **33,** 2335. (f) K. Maeda, J. Akimoto, Y. Kiyozumi and F. Mizukami, *J. Chem. Soc., Chem. Commun.*, 1995, 1033. (g) J. Liang and G. K. H. Shimizu, *Inorg. Chem.*, 2007, **46**, 10449. (h) J. M. Taylor, A. M. Mahmoudkhani and G. K. H. Shimizu, *Angew. Chem., Int. Ed.*, 2007, **46**, 795. (i) R. M. P. Colodrero, K. E. Papathanasiou, N. Stavgianoudaki, P. Olivera-Pastor, E. R. Losilla, M. A. G. Aranda, L. Leon-Reina, J. Sanz, I. Sobrados, D. Choquesillo-Lazarte, J. M. Garcia-Ruiz, P. Atienzar, F. Rey, K. D. Demadis and A. Cabeza, *Chem. Mater*. 2012**, 24**, 3780-379. (j) F. Costantino, A. Donnadio and M. Casciola, *Inorg. Chem.* 2012**, 51**, 6992-7000. (k) X. Z. Lin and Z. Y. Yuang, *Eur. J. Inorg. Chem.* 2012**,** 2661-2664. (l) A. Dutta, A. K. Patra and A. Bhaumik, *Microporous Mesoporous Mater*. 2012, **155**, 208-214. (m) D. P. Dong, L. Liu,Z. G. Sun, C. Q. Jiao, Z. M. Liu, C. Li, Y. Y. Zhu,K. Chen and C. L. Wang, *Cryst. Growth Des.* 2011**, 11**, 5346-5354. (m) P. O. Adelani and T. E. Albrecht-Schmitt, *J. Solid State Chem.* 2011**, 184**, 2368-2373. (n) J. Rocha, F.A. A. Paz, F. N. Shi, D. Ananias, N. J. O. Silva, L. D. Carlos and T. Trindade, *Eur. J. Inorg. Chem.* 2011, 2035-2044. (o) E. Brunet, H. M. H. Alhendawi, C. Cerro, C.; M. J. de la Mata, O. Juanes and J. C. Rodriguez-Ubis, *Microporous Mesoporous Mater*. 2011**, 138**, 75-85.

8. A. Clearfield, *Dalton Trans.*, 2008, 6089–6102.
9. R. Vaidhyanathan, A. H. Mahmoudkhani and G. K. H. Shimizu, *Can. J. Chem.*, 2009, **87**, 247–253.
10. M. Taddei, F. Costantino, A. Ienco, A. Comotti, P. V Dau and S. M. Cohen, *Chem. Commun.*, 2012, **49**, 1315–1317.
11. R. K. Mah, M. W. Lui and G. K. H. Shimizu, *Inorg. Chem.*, 2013, **52**, 7311–7313.
12. M. Taddei, F. Costantino, R. Vivani, S. Sabatini, S.-H. Lim and S. M. Cohen, *Chem. Commun.*, 2014, **50**, 5737–5740.
13. H. L. Ngo, A. Hu and W. Lin, *J. Mol. Catal. A Chem.*, 2004, **215**, 177–186.